

San Jose State University

From the Selected Works of Juana Vivó Acrivos

1988

Power Absorption of $Y_1Ba_2Cu_3O_{7-g}$ from 2 to 8 MHz near Zero Fields

Juana Vivó Acrivos, *San José State University*



Available at: https://works.bepress.com/juana_acrivos/140/

Power Absorption of $Y_1Ba_2Cu_3O_{7-\delta}$ from 2 to 8 MHz near Zero Fields

89

Power Absorption of $Y_1Ba_2Cu_3O_{7-\delta}$ from 2 to 8 MHz near Zero Fields

J.V. Acrivos, R. Ithnin, C. Bustillo, M. Chen Lei and D. Hellmoldt

San Jose' State University, San Jose' CA 95192

PACS Numbers: 7430C; 7470M;7470v

Abstract: We have prepared compounds with the nominal composition $Y_1Ba_2Cu_3O_{7-\delta}$ ($\delta \rightarrow 0$, usually identified by the Y, Ba, Cu stoichiometry: (1,2,3) and have characterized the materials (in addition to the usual X-ray diffraction and fluorescence) by EMF measurements in the electrochemical cell:

Cu/CuBr₂ (0.05 M in methanol)/(1,2,3)/Cu or Pt

versus temperature from 298 to 150 K. The superconducting transition temperatures were determined using the Meissner effect: in static magnetic fields by weight changes and, in radiofrequency fields from 2 to 8 MHz by the power absorption near magnetic fields $H = 0$. The observation of structure in the rf signals near $H = 0$ is discussed in light of the current theories that describe the superconductivity in these materials.

Introduction: The purpose of this work is to characterize the (1,2,3) superconductors by electrochemical measurements which can give information on the electronic processes in the ceramic and to determine the power absorption at radiofrequency fields when the skin depth due to the normal conductivity is of the order of the grain size. The accepted description of superconductivity in these ceramics is due to Ebner and Stroud (1985). The ac magnetic susceptibility can measure non-equilibrium properties caused by the "frustration" induced by the number of closed loops available for conduction in superconducting clusters. Then non-equilibrium phenomena are observed when the inverse relaxation times are greater than the rf-frequencies.

Experimental: The preparation of superconducting ceramics was carried out starting from reagent grade oxides. We follow the standard procedures, e.g., after twice grinding the reagent grade oxide mixture and firing it in alumina crucibles (in air at 840°C) the final sintering (in O_2 at 840°C) was carried out on thin pellets (of 1 cm radius and thickness ≤ 1 mm). The structure and composition were established by Cu $K\alpha$ X-ray diffraction and X-ray fluorescence using a Diano 800 system. Here the characteristic diffractions (013) and (110)+(103) near $2\theta = 32.8^\circ$; (020)+(006) and (200) near $2\theta = 46.5^\circ$ and (116) + (123) near $2\theta = 48.6^\circ$ are used to determine a $\approx 90\%$ purity for the material. The compressed pellets have a preferred alignment, showing only intense (005) and (006) diffractions. The electrochemical cell was constructed using Cu metal as one electrode in contact with a 0.05 M $CuBr_2$ solution in reagent

grade methanol and this was in contact with the (1,2,3) ceramic attached to a Cu electrode by clip-on pressure or to a Pt electrode by @Platinum Paste (Demetron). The data was independent of the electrode attached to the ceramic, indicating that the metal constituent of the electrode is the (1,2,3) ceramic. Zero EMF was measured when the green phase of the ceramic or a CuO pellet replaced the superconducting ceramic. The whole assembly was contained in a moisture tight cell with connections for the electrodes and a Copper Constantan thermocouple (calibrated at liquid nitrogen and Dry Ice acetone bath temperatures). This was immersed in a Dewar cooled by boiling liquid nitrogen. The EMF and temperature measurements were carried out using an hp 3455A digital voltmeter together with an hp 9435A computer system. The data for different samples are plotted in Figure 1 versus T and 1/T in order to deduce the thermodynamic properties of the cell. The value of T_C was determined for the plates used for the EMF measurements before and after each of the runs using a simple dc susceptibility balance with a calibrated copper constantan thermocouple cooled by boiling liquid nitrogen. The midpoint of the S-curve gave a transition temperature greater than or equal to 90 ± 2 K for all samples used. The rf measurements were made on 2 by 2 by 1 mm pellets covered with epoxy for protection against moisture and on oriented grains made from the latter. The value of T_C measured by plotting the rf amplitude versus T gave similar S curves with a midpoint at least 10 K above that for the dc measurements. Oriented powders ($d < 38 \mu m$) were obtained by grinding the pellets and passing them through a sieve and after mixing with 5 min epoxy, rods 3 cm long and 1 mm diameter were allowed to set in fields of 0, 1.35, 2 and 4 T for

Power Absorption of $Y_1Ba_2Cu_3O_{7.6}$ from 2 to 8 MHz near Zero Fields

at least 20 minutes. The alignment is shown in Figure 2. The data shown in Figures 3 and 4 were obtained using Varian V-4200 rf probes with and without field modulation together with a Bruker ER 200 magnet and lock-in detector system. The direct absorption and dispersion signals shown in Figure 4 were obtained by recording the output of the detector level (relative to a $\pm 20 \mu A$ leakage current introduced by resistive and inductive coupling paddles which undercouple and overcouple the cross coils, respectively) versus the sweep field in the Bruker magnet which was centered about zero field by applying 16 V to the rapid scan coils with an hp 6286A DC power supply. Lock-in detection at modulation frequencies of 400 Hz and 1.56 kHz was carried out using the Varian V4200 and the Bruker ER 200 lock-in detectors respectively. Distortion due to the large filling factors was ruled out by measuring an equally intense signal from a free radical reference which defined $H_z = 0 \pm 0.5$ Oe.

Discussion, EMF Measurements: The results in Figure 1 indicate that the reaction which describes the cell:



has constant enthalpy and entropy changes of:

$$\Delta H_{\text{cell}} = 29.7 \text{ kJ/mole} \pm 25\% \text{ and } \Delta S_{\text{cell}} = 212 \text{ J/mole/K} \pm 14\%$$

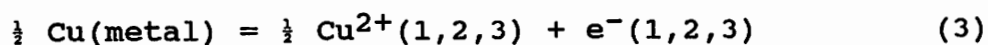
in the temperature interval 298 to 150 K. The high entropy change suggests that the reaction which represents this cell may be compared with that for the cell:



and the activity of the free electrons in the metal in ammonia solution is to be compared with that in the (1,2,3) ceramic, i.e., according to Schindewolf (1984):

$$\Delta S^\circ_{(e^-(am))} = 154 \pm 20 \text{ J/mole/K and } \Delta H^\circ_{(e^-(am))} = -95 \pm 10 \text{ kJ/mole}$$

for the metal in ammonia solutions. Since the change in entropy for the cell is comparable to the production of a solvated electron in metal in ammonia solutions the cell reaction can now be written as:



where the activity is $a = 1$ for the pure materials (i.e., standard states). This means that the cell EMF measures the activity of the conduction electrons in the ceramic and its temperature dependence. The large entropy change indicates that the metallic $e^-(1,2,3)$ have more states available to them than in the Cu metal. Also the different sign of ΔH_{cell} and $\Delta H^\circ_{(e^-(am))}$, indicates that the $e^-(1,2,3)$ are at a higher energy than in the metal whereas the opposite is true for the standard state of solvated $e^-(am)$. Solvation may explain the latter but the large entropy change may be of some importance for the theoretical description of these compounds.

RF Power Absorption: The power absorption at 9 GHz (with normal metal penetration depths of 5 microns) has been used as a measure of the transition to superconductivity according to Stankowski, Kahol, Dalal and Moodera (1987); Khachaturyan, Weber, Tejedor, Stacy and Portis, (1987) and Glarum, Marshall and Schneemeyer, (1988). At 2 to 8 MHz frequencies the normal penetration depths are greater than the

grain size (38 μm) in this work so that the entire sample is probed. The 7 kHz rf power absorption near zero magnetic fields has been explained by Jeffries et al., (1988) using the principles of non-linear electrodynamics in ceramic superconductors. This power absorption has been attributed to the spin-glass behavior diamagnetic susceptibility of superconducting clusters as described by Ebner and Stroud (1985). The dc and ac susceptibility:

$$\chi_{dc} = (M/H)_T \quad \text{and} \quad \chi_{ac} = (\partial M / \partial H)_T. \quad (4)$$

differ when $B \cdot nS / \phi_0 \geq 1$ ($\phi = Sn \cdot B$ is the flux through the loop of area S with unit normal n and, $\phi_0 = hc/2e$ is the quantum of flux in a superconductor, CGS units). Landau and Lifshitz (1960) and Ebner and Stroud (1985) define formal auxiliary quantities to express the magnetic properties: $M = \sum_{\langle ij \rangle} I_{ij} \frac{1}{2} (\mathbf{x}_i + \mathbf{x}_j) \cdot (\mathbf{x}_j - \mathbf{x}_i) / 2c$ is the magnetic moment of the cluster when I_{ij} is the superconducting current from grain i at \mathbf{x}_i to j at \mathbf{x}_j in Figure 2. The flux density $B = \mu_0 \langle h(\mathbf{x}_i) \rangle = \mu H$ defines the permeability μ . In a non superconducting host, the i th grain has an energy gap $\phi_i = \Delta_i \exp i\theta_i$, and is coupled via the host to other grains according to the Hamiltonian:

$$H = - \sum_{i,j} J_{ij} \cos(\theta_i - \theta_j - A_{ij}) \quad (5)$$

when $J_{ij} = hc I_{ij} / 2e$ is the coupling energy and the critical current between the two grains is $I_{ij} = I_c = \pi \Delta_i(T) / 2e R_{ij} \tanh(\Delta_i(T) / 2k_B T)$ when R_{ij} is the resistance between the two grains in the normal state. For identical grain coupling $A_{ij} = 2\pi \int_i^j \mathbf{A} \cdot d\mathbf{l} / \phi_0 = 2\pi / N$

$S_n \cdot B / \phi_0$ leads to "frustration" and magnetization jumps when $S_n \cdot B = N$ (Ebner and Stroud, 1985). In ceramics prepared similarly to ours, the magnetization deviates from linearity for $H > 5$ Oe (Zhang, Yan, Ma, Peng, Sun, Li, Wen, and Zhang, 1988) giving $\langle S \rangle \approx 4 \cdot 10^{-8}$ cm². The Meissner state does not exist above these fields and the new phenomena reported in Figure 4 must be explained on this basis. At microwave frequencies Portis, Blazey, Muller and Bednorz (1988) obtain critical fields $H^* = 0.05$ to 0.03 Oe. Also the decay of the signal observed by Warden, Baselgia, Berlowitz, Erhart, Senning, Stalder, Stefanicki, Portis and Waldner (1988, Figure 5) suggests that the relaxation rates in these ceramics are of the order of 10^3 s⁻¹ \ll 2 MHz and therefore non-equilibrium phenomena are to be expected. But we find that the cooling of the sample in zero field is important.

The tuned cross coil circuit in this work consists of a transmitter coil with axis along X shown in Figure 2 and a receiver coil with axis parallel to Y. Here the inductance L of the empty coil system is changed when a sample of rf susceptibility $\chi_{ac} = \chi'(w) - i\chi''(w)$ occupies a fraction η of the coil volume to $L(1 + 4\pi\eta\chi)$. The tuned cross coil circuit supplied by a constant current will develop across the receiver terminals a voltage proportional to the impedance:

$$Z = R(1 + 4\pi\eta\chi_{ac} - i/Q) / (1 + 4\pi i\eta Q\chi_{ac}) = R\{ (1 - 4\pi i\eta Q\chi_{ac}) / (1 + (4\pi\eta Q\chi_{ac})^2) - i/Q \} \quad (5)$$

where R is the shunt resistance of the circuit, the factor of merit

is $Q \approx 100$ and $\eta = .1$ to $.01$. As a result, a change in χ_{ac} with H produces a relative voltage variation of $\delta v/v \propto -4\pi\eta XQ/(1+(4\pi\eta QX)^2)$. Two paddles for magnetic coupling allow us to detect in principle both χ'' and χ' . With these paddles a leakage voltage V_L is added to δv so that the signal at the receiver coil is $|V_L + \delta v| - |V_L|$. The signal in phase with $\pm V_L$ will then be detected i.e., $\pm\chi'$ or $\pm\chi''$ as shown in Figure 4. We assume that $H_1 \sin \omega t$ is decomposed into two counter-rotating fields and that the detected absorption is from the field in phase with the superconducting current. The signal is determined by the magnetization $M_x = \text{re}\{2B_1 \chi_{ac} e^{i(\omega t - \pi/2)}\}$ along the x -direction and that induced in the receiver coil M_y at say an angle $\hat{y} \cdot \hat{x} = \pi/2 - \theta$, where resistive and inductive paddles select the value of θ , allowing for the detection of either χ' or χ'' according to the relation:

$$d M_y(t)/dt = d/dt\{M_x(\omega t - (\pi/2 - \theta))\} = \omega[\chi' \sin(\omega t + \theta) - \chi'' \cos(\omega t + \theta)]. \quad (7)$$

Portis, Blazey, Muller and Bednorz (1988) obtain the surface impedance in microwave fields to be $Z_p = -iX_0(1 + 2ifB/B_0)^{1/2}$ (fB/ϕ_0 is the density of free or weakly pinned fluxons and, X_0 and B_0 are parameters derived from the theory). B_0 is proportional to w times an effective penetration distance squared and $B_0/f = 6$ Oe fits the data in Figure 4 in the region $H = \pm 5$ Oe, when B is set equal to H and, the amplitude ratios $|\chi''|/|\chi'| = 5$ at both 9 GHz and 2 MHz, suggest that B_0/f is independent of w .

The sample cooling can lead to non-equilibrium processes. In both

oriented and randomly oriented grains, the most important observation is that (whether the circuit is tuned to detect χ'' or χ') there are two signals associated with the superconductor, one which depends on the phase of the coupling between the transmitter and receiver coils, i.e., the sign of V_L and another independent of it. In powders oriented at 2 T, we find that when the samples are cooled in 0 ± 0.5 Oe at an orientation $\alpha = \mathbf{H}_z \cdot \mathbf{H}_0 = 0$, where \mathbf{H}_0 is the field orientation at which the epoxy matrix was set, $d\chi''/dH$ changes with the sign of V_L only at the cooling orientation (Figure 3a). After the sample is rotated in the magnetic field there appear to be two signals, one which is independent of the sign of V_L , i.e., it is independent of the phase of the coupling between the transmitter and receiver coils with a very small component ($\approx 15\%$) which varies with the phase of the coupling. When the same sample was cooled in 0 ± 0.5 G but $\alpha = \pi/2$, the effect disappears. This is the first time that such an effect has been observed and it is introduced by moving the sample in the magnetic field of 20 Oe. If \mathbf{H}_0 is assumed to align the grains with $\mathbf{c} \parallel \mathbf{H}_0$ one is tempted to explain the phase coupling independent signals as arising from current loops introduced on rotation in a magnetic field.

Conclusions: We have tried to obtain physical insight into the thermodynamic properties of the (1,2,3) superconductors above the transition temperature T_C and, on the motion of the electrons in the superconducting state which leads to critical phenomena dependent on the magnitude and orientation of the external magnetic field. The thermodynamic measurements indicate that the activity of the normal

conduction electrons in (1,2,3) gives rise to an EMF governed by the increase in entropy and enthalpy from the normal conduction electrons in Cu metal. In the superconducting state, rf measurements have shown that the surface impedance in the superconductor leads to a power absorption near zero magnetic fields which is made up of two different types of signals. The rf signal which changes sign with the phase of the coupling may be associated with the motion of flux versus H (Portis et al, 1988). The fine structure shown in Figure 5 is observed above fields of 150 Oe and the broad signal near $H = 0$ decreases as the magnitude of H_0 increases from 0 to 1.35 to 2 to 4 T. If the Portis et al., law for the field spacing of microwave absorption versus H in a single crystal (with junctions in the {110} plane: $H \cos\theta = \pm(p+\frac{1}{2})\Delta H$, where $S \cos\theta \Delta H / \phi_0 = 1$ when S is the junction area and $\theta = [110] \wedge H$) is obeyed, even if there are several orientations present for the Josephson Junctions, the first two lines about $H = 0$ should give the magnitude of S when $\theta = 0$. The fine structure spacing of $\Delta H = 1.2 \pm 0.1$ Oe symmetric about $H = 0$ Oe. when $\alpha = 0$ is used to ascertain the magnitude of S for Josephson Junctions along the ab planes when $d+2\lambda = 2 \mu\text{m}$ micron in Figure 2. This gives a grain size of $\approx 10 \mu\text{m}$ which puts three to four grains into the $38 \mu\text{m}$ oriented powders.

Acknowledgements: This work was carried out under the auspices of NSF Grant DMR 8612094. RI wishes to thank the government of Malasia for a graduate fellowship CB wishes to thank the ACS minority program for a summer fellowship (1987) and JVA wishes to thank NSF grant VPW RII8700099 for encouragement during the academic year 1987-1988, received in many ways, specially from long talks at UC Berkeley with Dr. M.P. Klein and Professors C. Jerffries and A. Portis.

Bibliography:

- Blazey KW, Portis AM and Bednorz JG, 1988, *Solid State Comm.*, **65**, 1153
- Blazey KW, Portis AM, Muller KA, Bednorz JG and Holtzberg, 1988, *Physica C* **153-155**, 56
- Ebner C and Stroud D, 1985, *Phys. Rev.* **B31**, 165
- Farrell DE, Chandrasekhar BS, DeGuire MR, Fang MM, Kogan VG, Clem DK and Finnemore DK, 1987, *Phys. Rev.* **B36**, 4025
- Glarum SH, Marshall JH and Schneemeyer LF, 1988 *Phys. Rev.* **B37**, 7491
- Kachaturyan K, Tejedor P, Stacy AM and Portis AM, 1987, *Phys. Rev.* **B36**, 8309
- Landau LD and Lifshitz EM, "Electrodynamics of Continuous media", Pergamon, London, 1960
- Jeffries C, Lam QH, Kim Y, Bourne LC and Zetl A., 1988, *Phys. Rev.*, **B37**, 9840
- Kittel C, 1986, "Introduction to Solid State Physics", J.Wiley and Sons, Inc., 6th ed.
- Portis A and Blazey KW, 1988, *Solid State Communications*, in press
- Tinkham M, 1975, "Introduction to Superconductivity", McGraw Hill, NY
- Schindewolf U, 1984, "Physics and Chemistry of Electrons and Ions in Condensed Matter", Acrivios, JV, Mott, NF and Yoffe, AD ed., D. Reidel, p361
- Stankowski J, Kahol PK, Dalal NS and Moodera JS, 1987, *Phys. Rev.* **B36**, 7126
- Warden M, Baselgia L, Berlowitz D, Erhardt P, Senning B, Stalder M, Stefanicki G, Portis AM and Waldner F, 1988, **24th Congress Ampere**, in press.

List of Figures:

Figure 1: EMF measurements for the cell $Cu/CuBr_2(0.05 \text{ M in methanol})/(1,2,3)$. (a) E/T versus $1/T$ and (b) E versus T .

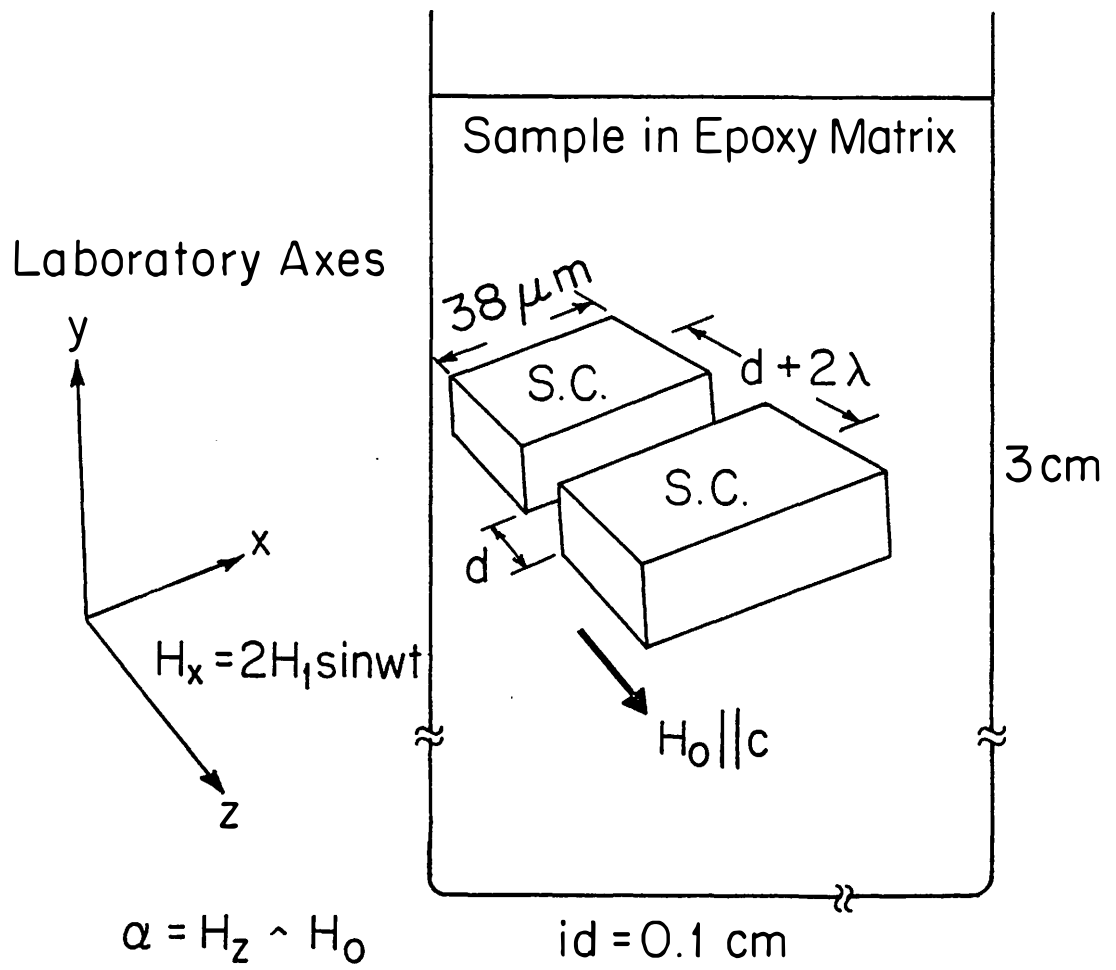
Figure 2: Orientation of aligned (1,2,3) grains in the laboratory axes. $38 \mu\text{m}$ grains dispersed in an epoxy matrix were aligned and set at room temperature in $H_0 = 0, 1.35, 2$ and 4 T . A sample is always cooled from room temperature to 77 K at $H_z = H_m = H_1 = 0 \pm 0.5 \text{ Oe}$. $H_z = 0$ was determined by the esr absorption of a free radical.

The orientation is for dislocations that occur in planes normal to the c -axis. Other orientations are possible, e.g., along the $\{110\}$ planes as observed by Portis et al., 1988. The sample can be rotated about the Y axis to vary $\alpha = H_z \hat{H}_0$. X-ray diffraction of similarly prepared samples (Farrell, Chandrasekhar, DeGuire, Fang, Kogan, Clem and Finnemore, 1987) show that there is a preferred alignment with $c \parallel H_0$.

Figure 3: RF absorption at $\nu = 2 \text{ MHz}$ and 77 K of oriented grains of samples cooled at different orientations α shown in Figure 2: (a) Sample cooled at $\alpha = 0$ but no rotation in H_z . (b) Sample cooled at $\alpha = 0$ and rotated to $\alpha = \pi/6$ at $H_z = 20 \text{ Oe}$. (c) Sample cooled at $\alpha = \pi/2$ and rotated to $\alpha = 0$ at $H_z = 20 \text{ Oe}$. $H_m = H_{m,\text{max},1.56\text{kHz}} = 2 \text{ Oe}$.

Figure 4: RF absorption at $\nu = 2\text{MHz}$ and 77 K of grains in a ceramic pellet at random orientation: (a) Circuit tuned to detect χ'' . (b) Circuit tuned to detect χ' . No modulation.

Figure 5: Fine structure observed on oriented samples for different values of H_0 , at $\nu = 8 \text{ MHz}$ and 77 K : (a) Samples oriented at $H_0 = 2 \text{ T}$. (b) Samples oriented at $H_0 = 4 \text{ T}$. The spacing $\Delta H = 1.2 \pm 0.1 \text{ Oe}$ symmetric about $H_z = 0$ suggests that the rf absorption follows the Portis et al. law for a single crystal. $H_m = H_{m,\text{max}}/45$.



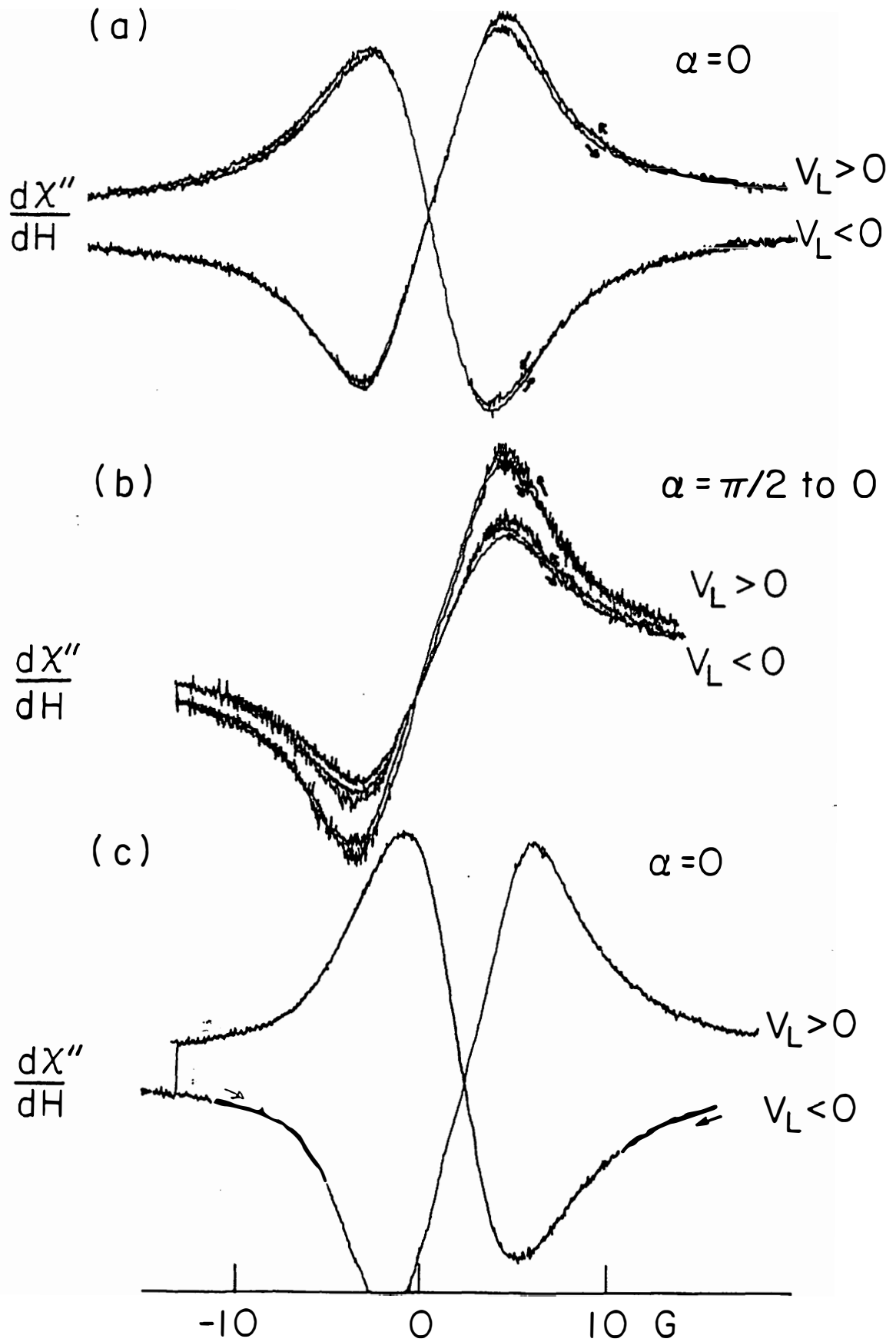


Figure 3:

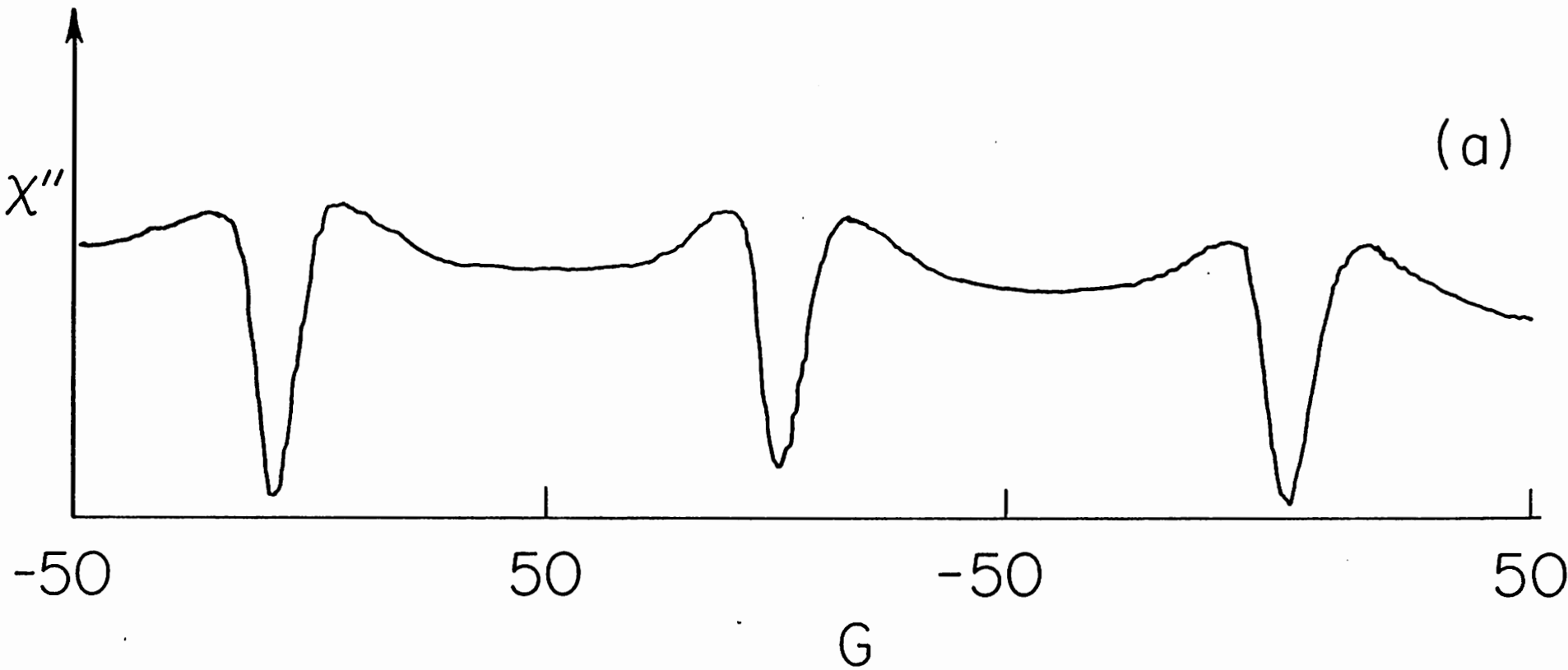
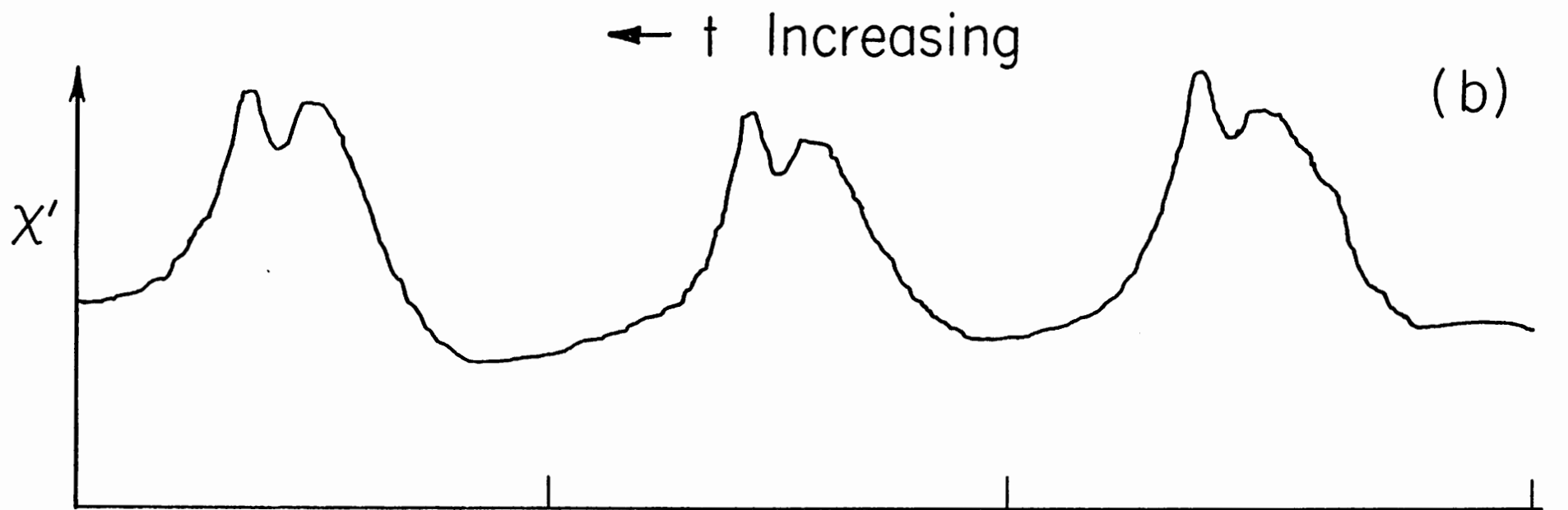


Figure 4

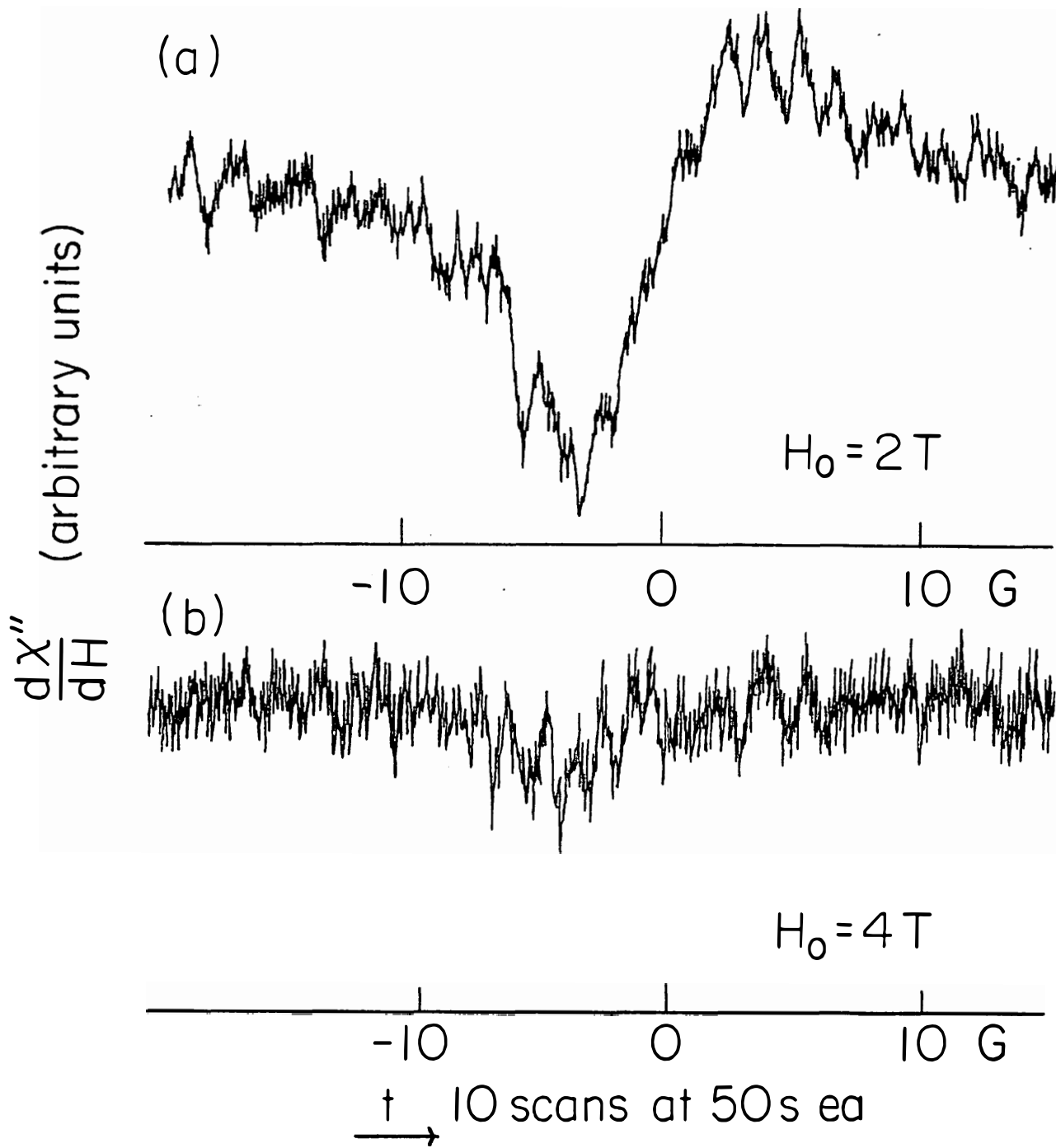


Figure 5.